

# *B* Physics with the CDF Run II Upgrade

FERMILAB-Conf-95/408-E

Fritz DeJongh<sup>a</sup><sup>a</sup>Fermilab M.S. 318, P.O. Box 500, Batavia IL 60510

We summarize Run I results relevant to an analysis of the CP asymmetry in  $B \rightarrow J/\psi K_s$ , the CDF upgrade plans for Run II, and some of the main *B* physics goals related to the exploration of the origin of CP violation.

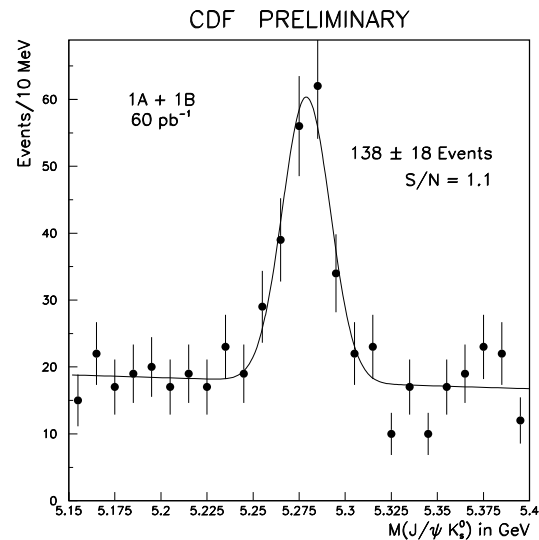
## 1. INTRODUCTION

During the Run I data taking period, from 1992 through 1995, CDF has acquired  $110 \text{ pb}^{-1}$  of  $p\bar{p}$  collisions at a center of mass energy of 1800 GeV. This data has provided many results on *B* physics [1], and provides a basis for extrapolating to Run II, which is scheduled to start in 1999 after major upgrades to both the accelerator and detector.

We present herein a summary of Run I results relevant to an analysis of the CP asymmetry in  $B \rightarrow J/\psi K_s$ , the CDF upgrade plans for Run II, and some of the main *B* physics goals related to the exploration of the origin of CP violation.

## 2. TAGGED $B \rightarrow J/\psi K_s$ IN RUN I

In the first  $60 \text{ pb}^{-1}$  of Run I, as shown in Figure 1, we have observed  $140 B^0 \rightarrow J/\psi K_s$  events with signal-to-noise better than 1:1. We obtained this sample with a dimuon trigger that required both muons to have transverse momentum ( $P_T$ ) greater than 2.0 GeV. To obtain the CP asymmetry we must tag the flavor of the *B* meson at the time at which it was produced. Work is under way to use a combination of Run I data and Monte Carlo to establish the "effective tagging efficiency"  $\epsilon(1 - 2w)^2$ , where  $\epsilon$  is the tagging efficiency and  $w$  is the mistag fraction, for a variety of algorithms. We currently have results [2] for two methods, Jet Charge and Muon tagging, for a total effective tagging efficiency of  $\approx 2\%$ . These results indicate that an order of magnitude improvement in the statistical uncertainty on the CP asymmetry will lead to a competitive measurement in Run II.

Figure 1.  $B_d \rightarrow J/\psi K_s$  signal.

## 3. ACCELERATOR IMPROVEMENTS FOR RUN II

A project called Fermi III is underway [3] to upgrade the Fermilab accelerator complex to produce an order of magnitude higher luminosity in the Tevatron. The luminosity in Run I was limited by the antiproton current. The largest component of Fermi III is to replace the Main Ring, which is housed in the same tunnel as the Tevatron and provides the acceleration stage just prior to the Tevatron, with the Main Injector, which will be housed in a separate and new tunnel. The

Main Injector will provide for higher proton intensity onto the antiproton production target, and larger aperture for antiproton transfer into the Tevatron. Combined with improvements to the antiproton cooling system, the antiproton stacking rate will increase by over a factor of three to  $17 \times 10^{10}$  per hour.

The Tevatron schedule and some basic parameters are shown in Figure 2. Our physics projections for Run II assume  $2 \text{ fb}^{-1}$  of integrated luminosity.

#### 4. DETECTOR IMPROVEMENTS FOR RUN II

The CDF detector is being upgraded to handle an order of magnitude higher luminosity, and 132 ns bunch spacing [4]. The main goal is to maintain detector occupancies at Run I levels, although many of these upgrades also provide for qualitatively improved detector capabilities.

##### 4.1. Tracking Upgrades

The efficiency of the current tracking system would be significantly degraded at luminosities of  $10^{32} \text{ cm}^{-2}\text{sec}^{-1}$ : Primary track efficiency would drop by 10%, and  $K_s$  efficiency would drop by 60%. A three part tracking upgrade is being planned to recover this efficiency:

- A Central Straw Tracker (CST) will consist of 4 axial and 4 stereo superlayers of 8 to 12 straws each at radii of 50 to 140 cm.
- An Intermediate Scintillating Fiber Tracker (IFT) will consist of six stereo and six axial layers of 500 micron diameter scintillating fibers read out by VLPCs.
- A new Silicon Vertex Detector (SVX II). The SVX II will consist of 5 layers of double sided silicon from radii of 2.9 to 10 cm, arranged in 5 axial layers, 2 small angle ( $1.2^\circ$ ) stereo layers, and 3  $90^\circ$  stereo layers.

Since each of these detectors can be read out in less than 132 ns, occupancies will be held to Run I levels up to luminosities of  $3 \times 10^{32} \text{ cm}^{-2}\text{sec}^{-1}$  at 132 ns bunch spacing. Furthermore, each detector is potentially a stand-alone 3D tracker, pro-

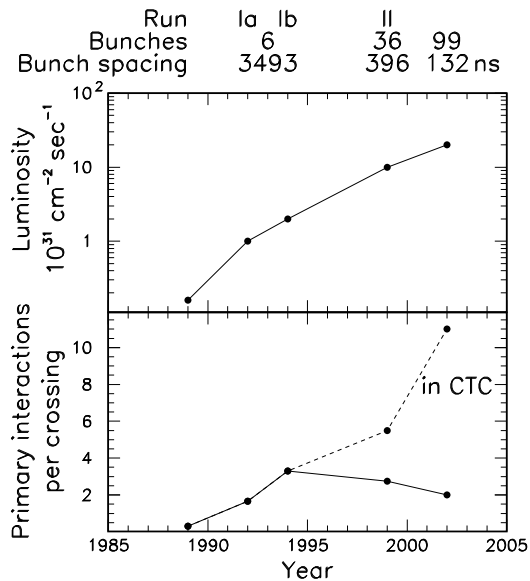


Figure 2. The Tevatron schedule. As the luminosity increases, the number of bunches increases, and the number of primary interactions per bunch crossing remains at Run I levels. The current Central Tracking Chamber (CTC) has a drift time of 750 ns, and thus at any given time is occupied by events from more than one bunch crossing.

viding for greater redundancy in pattern recognition.

In addition to maintaining efficiency, these upgrades provide for new tracking capabilities: Precision vertexing in 3 dimensions, tracking to  $|\eta| < 2$  and tracking down to  $p_T > 100 \text{ MeV}/c^2$ .

##### 4.2. Time of Flight

We are planning for a Time of Flight system consisting of 3 m long  $4 \times 4$  cm scintillator blocks placed at a radius of 1.4 m (inside the solenoid) and read out with mesh dynode photomultiplier tubes. The 4 cm width results in less than 20% confusion from multiple hits and other noise sources. We expect 100 to 125 ps time resolution, for  $> 2\sigma K/\pi$  separation in the momentum range

from 0.3 to 1.6 GeV/c. This momentum range includes 55% of kaons potentially useful for flavor tagging.

### 4.3. Trigger and DAQ system

CDF is planning for a trigger and DAQ upgrade to allow for higher data rates while increasing the sophistication of the trigger decision, as summarized in Figure 3. Data is stored in a 42 cell pipeline while awaiting the Level 1 trigger decision, and can be transferred to Level 2 without halting Level 1. Information available for the Level 1 decision will include calorimetry clusters, CST tracks with  $p_T > 1.5$  GeV/c<sup>2</sup>, and electron and muon identification. At Level 2, SVX II information will also be available, and DEC Alpha based processors allow for programmable algorithms. A commercial switch will be used to assemble events into the Level 3 processors where a full event reconstruction will be performed for the final trigger decision.

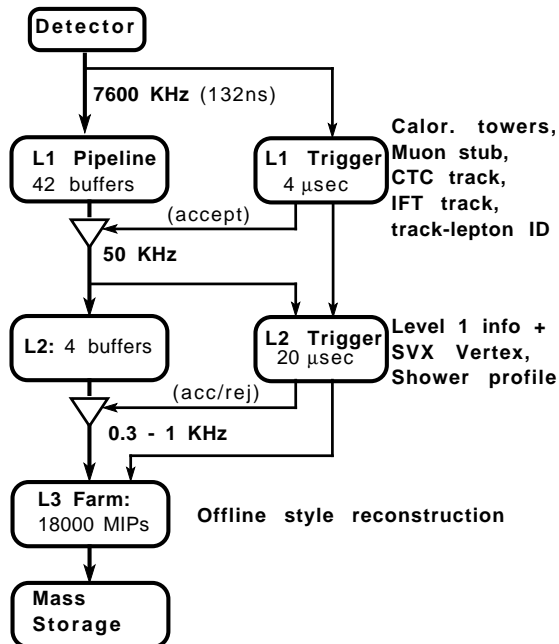


Figure 3. Trigger and data acquisition flow.

## 5. B PHYSICS EXPECTATIONS FOR RUN II

The challenge for  $B$  physics in Run II is to develop efficient trigger algorithms for key final states, and efficient flavor tagging algorithms. In this section, we discuss possibilities for flavor tagging, measurements of  $\sin(2\beta)$ ,  $\sin(2\alpha)$ ,  $B_s$  mixing, and the observation of rare decay modes. Topics not discussed here include [5]: The CP angle  $\gamma$  [6], study of exclusive  $b \rightarrow u$  semileptonic decays, measurement of  $V_{cb}$  in semileptonic  $\Lambda_b$  decays, and  $B_c$  spectroscopy.

### 5.1. Flavor tagging

As discussed in Section 2 we currently have results for two flavor tagging methods, jet charge and muon tagging, for a total effective tagging efficiency of almost 2%. Our goal for Run II is to attain the following effective tagging efficiencies from various algorithms:

- 2% from lepton tagging, using electrons as well as muons, and additional coverage planned for lepton identification in Run II.
- 2% from same-side tagging, which exploits the charge correlation of the pions produced in the fragmentation process along with the  $B$  meson [7]. For the  $B_s$  case, the charge correlation of kaons identified in the time-of-flight system may result in a tagging efficiency of 5%.
- 3% from kaon tagging, using tracks with high impact parameter identified as kaons in the time of flight system.
- 4% from a jet charge algorithm exploiting 3D vertexing information from the SVX II, and stand-alone tracking information from the SVX II and Intermediate Fiber Tracker.

While work is in progress to evaluate all these algorithms using current data, for now we assume an 8% flavor tagging efficiency for  $B_d$  mesons, and 11% for  $B_s$  mesons.

### 5.2. CP Asymmetry in $B_d \rightarrow J/\psi K_s$ : $\sin(2\beta)$

With a large branching ratio and distinctive trigger signature, the decay mode  $B_d \rightarrow J/\psi K_s$  is the leading candidate for the initial observation of

CP violation in the  $B$  system. Furthermore, the extraction of  $\sin(2\beta)$  from this asymmetry is essentially free of hadronic uncertainties. The current Standard Model predictions for  $\sin(2\beta)$  are  $\sin(2\beta) > 0.17$  [8] and  $\sin(2\beta) = 0.65 \pm 0.12$  [9].

As discussed in Section 2, CDF in Run I has reconstructed  $\approx 2 J/\psi K_s$  events per  $\text{pb}^{-1}$ , using a dimuon trigger with a  $p_T$  threshold of 2.0 GeV/c on each muon. Improvements for Run II include lowering the trigger  $p_T$  threshold to 1.5 GeV/c per muon, improving the muon coverage, and using the channel  $J/\psi \rightarrow e^+e^-$ . Our goal for Run II is to reconstruct 10  $B^0 \rightarrow J/\psi K_s$  events per  $\text{pb}^{-1}$ , for a yield of 20,000 events assuming  $2 \text{ fb}^{-1}$ . We also expect to achieve much improved signal-to-noise by using the improved capability and coverage of the SVX II, but have conservatively assumed  $S/N = 2:1$ . Assuming an effective tagging efficiency of 8%, we find an uncertainty on  $\sin(2\beta)$  of 0.07.

In addition to the above expectation of 20,000  $B^0 \rightarrow J/\psi K_s$  events in  $2 \text{ fb}^{-1}$ , the  $B^0 \rightarrow J/\psi K_s$  yield can increase by employing (a) the increased tracking coverage and (b) new ways of triggering, such as requiring one lepton and one additional track with large impact parameter. While speculative, an additional factor of four or more in the number of reconstructed  $B^0 \rightarrow J/\psi K_s$  events may be possible.

### 5.3. CP Asymmetry in $B_s \rightarrow J/\psi\phi$

Within the Standard Model, the CP asymmetry in  $B_d \rightarrow J/\psi K_s$  measures the weak phase of the CKM matrix element  $V_{td}$ , while the CP asymmetry in  $B_s \rightarrow J/\psi\phi$  measures the weak phase of the CKM matrix element  $V_{ts}$ , which is expected to be very small. As emphasized by Y. Nir [10], and Helen Quinn at this workshop, the channel  $B_s \rightarrow J/\psi\phi$  may therefore provide a signature for a source of CP violation beyond the Standard Model. With the same trigger improvements as for  $B_d \rightarrow J/\psi K_s$ , we expect 12000  $B_s \rightarrow J/\psi\phi$  events in Run II.

The magnitude of a CP asymmetry in  $B_s \rightarrow J/\psi\phi$  decays would be modulated by the frequency of  $B_s$  oscillations. Thus, for a meaningful limit, we must be able to resolve  $B_s$  oscillations. If we neglect resolution effects, we can expect a

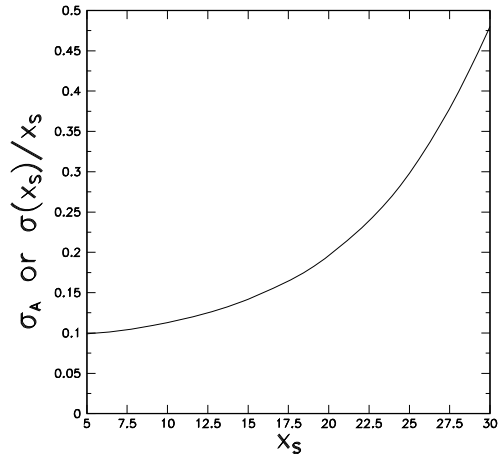


Figure 4. The uncertainty on the CP asymmetry for  $B_s \rightarrow J/\psi\phi$  (or the relative uncertainty on  $x_s$ ) as a function of the  $B_s$  mixing parameter  $x_s$

precision on the asymmetry of  $\pm 0.09$ . However, resolution effects smear the oscillations and produce an additional dilution. Our experience in Run I shows that if we determine the primary vertex event-by-event, the proper lifetime resolution for fully reconstructed  $B$  decays is  $\approx 30 \mu\text{m}$ . Figure 4 shows our expected precision on the asymmetry as a function of  $x_s$ . There will be an additional dilution if the  $J/\psi\phi$  final state is not a pure CP eigenstate.

### 5.4. CP Asymmetry in $B^0 \rightarrow \pi^+\pi^-$ : $\sin(2\alpha)$

A measurement of  $\sin(2\alpha)$  in conjunction with  $\sin(2\beta)$  provides powerful constraints on the unitarity triangle [11]. The greatest challenge in this measurement is the trigger requirement at a luminosity of  $1 \times 10^{32} \text{ cm}^{-2} \text{ sec}^{-1}$ . Our plan (described in detail in [12]) consists of

1. At Level-1: Require two tracks with  $P_T > 2$  GeV/c, imposing  $\Delta\phi$  cuts on opposite sign track pairs.

2. At Level-2: Require an impact parameter  $> 100 \mu\text{m}$  for each track.
3. At Level-3: Use the full event information for the final decision.

After additional analysis requirements we expect  $\approx 5 B^0 \rightarrow \pi^+\pi^-$  events per  $\text{pb}^{-1}$ . Due to the impact parameter cuts, the proper lifetime distribution starts at  $\approx 1.5$  lifetimes, and therefore the dilution of the CP asymmetry due to mixing of the signal  $B$  before it decays will be 0.82, rather than 0.47 as we assumed for  $\sin(2\beta)$ .

To measure the CP asymmetry in  $B^0 \rightarrow \pi^+\pi^-$  events one needs to determine the fraction of the signal from  $B_d \rightarrow K^+\pi^-$ ,  $B_s \rightarrow K^-\pi^+$  and  $B_s \rightarrow K^-K^+$  decays. This can be done using invariant mass and  $dE/dx$  distributions in the high statistics untagged sample. Figure 5 displays the expected mass distribution for the combination of the above four signals, assuming a pion mass assignment for all tracks [12]. The  $B_d \rightarrow \pi^+\pi^-$  and  $B_d \rightarrow K^+\pi^-$  peaks are separated by  $40 \text{ MeV}/c^2$ , while we expect a mass resolution of  $\approx 28 \text{ MeV}/c^2$ . As in Run I, we also expect  $K/\pi$  separation from  $dE/dx$  in the CST of better than  $1\sigma$ . Any CP asymmetry in the  $K\pi$  background component can be determined from the ratio of numbers of  $K^-\pi^+$  and  $K^+\pi^-$  events in the untagged sample. Any CP asymmetry in the  $K^+K^-$  background component would be modulated by the  $B_s$  mixing frequency rather than the  $B_d$  mixing frequency. Therefore, the CP asymmetry in the tagged sample in conjunction with a fit to the untagged sample can yield the CP asymmetry for  $B^0 \rightarrow \pi^+\pi^-$ .

Another issue for this analysis is the combinatorial background under the  $B$  peak. We can estimate this background level detector using a sample of high  $E_T$  electron triggers from Run I. In the case that the electron results from the semileptonic decay of a  $B$  hadron, we can search for the other  $B$  in the event to decay to  $\pi^+\pi^-$ . Using standard cuts on the decay vertex and the isolation of the two-track combination, we obtain an observed background,  $N$ , comparable to the expected signal,  $S$  (less than one event), for  $P_T > 4 \text{ GeV}/c$  on each track:  $S/N \approx 1 : 1$ . Lowering the  $P_T$  threshold to  $2 \text{ GeV}/c$  will allow us to double

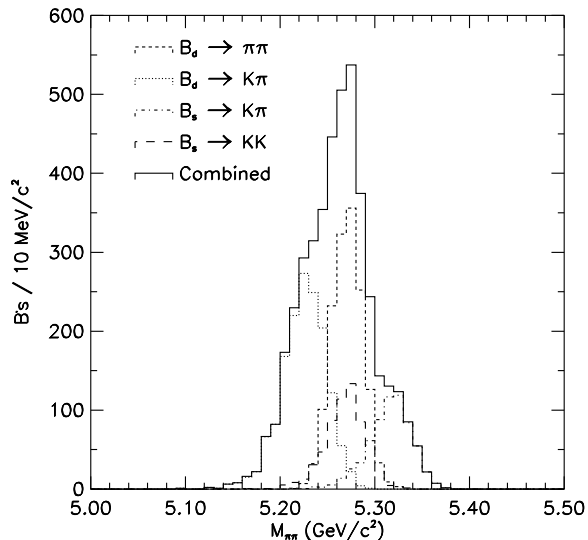


Figure 5. Mass distribution for the combination  $B^0 \rightarrow \pi^+\pi^-$ ,  $B_d \rightarrow K^+\pi^-$ ,  $B_s \rightarrow K^-\pi^+$  and  $B_s \rightarrow K^+K^-$  assuming a pion mass assignment for all tracks.

our efficiency. We expect to do this with the Run II detector while maintaining  $S/N$  better than 1:1 by exploiting the 3D information from the SVX II and optimizing cuts.

The final issue related to the extraction of the angle  $\alpha$  from the measured CP asymmetry in  $B_d \rightarrow \pi^+\pi^-$  is the extraction of possible penguin contributions in addition to the tree diagram which is expected to dominate this decay mode. We can estimate this penguin contamination, and thus extract  $\alpha$ , from a combination of experimental measurements and theoretical inputs. In particular, a time-dependent analysis yields a measurement of the amplitude as well as the phase of the CP asymmetry, which oscillates with the mixing frequency. This latter phase would be zero in the absence of a penguin contribution. In addition, we use the average branching ratio  $(Br(B^0 \rightarrow \pi^+\pi^-) + Br(\bar{B}^0 \rightarrow \pi^+\pi^-))/2$ . This quantity can be extracted from untagged  $B_d \rightarrow \pi^+\pi^-$  decays and will therefore have a very small

error. Other ingredients are the value of  $Br(B \rightarrow \pi \ell \nu)$  and some theoretical input such as the magnitude of the tree diagram given  $Br(B_d \rightarrow \pi^- \ell \nu)$ . As an example, if the penguin amplitude,  $A_p$ , is small compared to the tree amplitude,  $A_t$ , (say,  $A_p/A_t = 0.07$  as predicted by Deshpande *et al.* [13]) the extraction of  $\alpha$  is relatively easy, and the theoretical constraints can be relatively crude. If  $A_p/A_t \approx 0.2$ , this becomes more challenging, but feasible. A detailed analysis can be found in reference [14].

In conclusion, assuming a flavor-tagging efficiency of 8% as for the  $J/\psi K_s$  case, and a conservative  $S/N = 1/4$ , we expect an overall uncertainty on  $\sin(2\alpha)$  of  $\pm 0.10$ .

### 5.5. Measurement of $|V_{td}/V_{ts}|$

The CDF  $B$  physics goals for Run II include observation of the time dependence of  $B_s$  and  $B_d$  mixing, observation of exclusive radiative penguin decays, and the observation of a lifetime difference  $\delta\Gamma$  between the CP eigenstates of the  $B_s$  meson. The ratio of  $B_d$  to  $B_s$  mixing parameters,  $x_d/x_s$ , is proportional to  $|V_{td}/V_{ts}|^2$ . The matrix elements for  $B_d$  and  $B_s$  mixing are related by SU(3), allowing the cancellation of many theoretical uncertainties in the ratio. Similarly, in the absence of long distance effects, the ratio of decay rates  $B(B \rightarrow \rho\gamma)/B(B \rightarrow K^*\gamma)$  is proportional to  $|V_{td}/V_{ts}|^2$ . Again, since these final states are related by SU(3), many theoretical uncertainties cancel in the ratio.

A smaller value of  $|V_{td}/V_{ts}|$  implies a larger value of  $x_s$ , and a smaller rate for  $B \rightarrow \rho\gamma$ , and therefore both of these measurements become more difficult. However, the lifetime difference  $\Delta\Gamma_s$  is proportional to  $x_s$ , and therefore this measurement becomes easier. Although the theoretical uncertainties on  $\Delta\Gamma_s$  are larger, the combination of the three types of measurements discussed in this section should allow CDF to measure  $|V_{td}/V_{ts}|$  over the full range permitted by the standard model.

#### 5.5.1. $B_s$ Mixing

ALEPH has shown that  $x_s > 8.8$  [15], implying that  $x_s$  must be measured by fitting the time-dependent oscillation of the  $B_s$ . For the

Run Ia  $B_s$  lifetime measurement [16], CDF reconstructed 70  $B_s \rightarrow D_s \ell \nu$  events. For Run II, triggering and reconstruction of this channel with very high statistics is straightforward, and we expect  $\approx 10^5$  events. Due to the unreconstructed neutrino, knowledge of the  $B$  momentum limits the measurement to values of  $x_s < \sim 11$ . However, improvements in the analysis technique may result in an improved momentum resolution. For example, 3D vertexing allows a determination of the four-momentum of the missing neutrino, although with a quadratic ambiguity.

For fully reconstructed decays, the  $x_s$  reach is limited by vertexing resolution, as discussed in section 5.3. In order to determine the flavor of the  $B_s$  at the time of the decay this measurement requires events of the type  $B_s \rightarrow D_s n \pi$ . The challenge for CDF is to trigger on, and isolate from background, signals of this type. We note that the presence of a time-of-flight system in CDF should significantly improve the reconstruction efficiency by allowing efficient selection of kaons and rejection of pions at low  $P_T$ , where the backgrounds are largest.

One strategy is to trigger on a single lepton ( $e$  or  $\mu$ ), which will serve as the flavor tag, and then reconstruct  $B_s$  decays in this sample [17]. For a 6 GeV lepton threshold in Run II, there will be  $\sim 2 \times 10^3$   $B_s$  mesons that have decayed within the CDF fiducial volume to the modes  $B_s \rightarrow D_s + \pi$  and  $B_s \rightarrow D_s + 3\pi$  with  $D_s \rightarrow \phi\pi$  or  $D_s \rightarrow K^{*\pm}K^\mp$ . It is not yet known how many of these may be reconstructed with good signal-to-noise. It is likely that the lepton trigger threshold will be lower, and also that some of the decay products of the  $B_s$  will be included in the trigger requirement as well.

Another strategy is to use a fully hadronic trigger, as for  $B \rightarrow \pi^+\pi^-$ , in which case all tagging techniques may be applied. The final states of the  $B_s$  we are trying to reconstruct are produced an order of magnitude more frequently than  $B \rightarrow \pi^+\pi^-$ . More work is needed to design such a trigger; one possibility is a two-track trigger optimized for  $\phi \rightarrow K^+K^-$ .

Although we do not have a solid projection of how many events we will reconstruct, we show in Figure 4 our precision on  $x_s$  if we succeed in re-

constructing 2000 events from fully hadronic triggers, with an effective tagging efficiency of 11%, or equivalently, 800 events reconstructed in events with a lepton trigger.

### 5.5.2. Radiative $B$ Decays

Measurements of radiative  $B$  decays at CLEO sets an upper bound on  $|V_{td}/V_{ts}|$  of 0.76 [19]. CDF has already installed a trigger to collect radiative penguin decays. The limited bandwidth available in the current trigger and data acquisition system require the trigger to have quite high thresholds (10 GeV photon plus two 2 GeV tracks). The expected yield with this trigger is  $\approx 20 \gamma K^*$  events per  $100 \text{ pb}^{-1}$ . In Run II, we expect to lower the photon  $E_t$  threshold to 5 GeV and the track  $P_t$  threshold to 1.5 GeV, with a resulting yield of  $\sim 135$  events per  $100 \text{ pb}^{-1}$  or  $\sim 2700$  for  $2 \text{ fb}^{-1}$ .

The mass resolution of the reconstructed  $B$  is dominated by the resolution on the photon energy and is  $\sim 140 \text{ MeV}$ . We have studied our ability to reject combinatorial background using Run 1A photon data and have studied with Monte Carlo the discrimination against  $B \rightarrow K^* \pi^0$  and  $\rho \pi^0$  and from higher multiplicity penguin decays. These backgrounds are manageable. The mass resolution is not adequate to separate  $\gamma \rho$  from  $\gamma K^*$  on an event-by-event basis (see Figure 6); however, a statistical separation is possible. In addition, the CTC dE/dx system should provide  $1\sigma$   $K$ - $\pi$  separation in the momentum range of interest.

These radiative  $B$  decays can also be observed using converted photons. The probability for a photon to convert ( $\sim 5\%$ ) will be offset by a lower photon  $E_t$  threshold. Also, the mass resolution is  $\sim 5$  times better than for the signals with unconverted photons, allowing a cleaner separation between  $B \rightarrow \gamma K^*$  and  $B \rightarrow \gamma \rho$ .

At the Tevatron it is possible to study  $B_s$  penguin decays as well. Information on  $|V_{td}/V_{ts}|$  can be obtained in the same manner as above from studying the ratio of  $B(B_s \rightarrow \gamma K^*)/B(B_s \rightarrow \gamma \phi)$ . The size of the  $B_s$  penguin sample is expected to be 1/2 to 1/3 the size of the  $B_d$  sample. Comparison of the two results would help constrain the size of the long distance contributions to the decays.

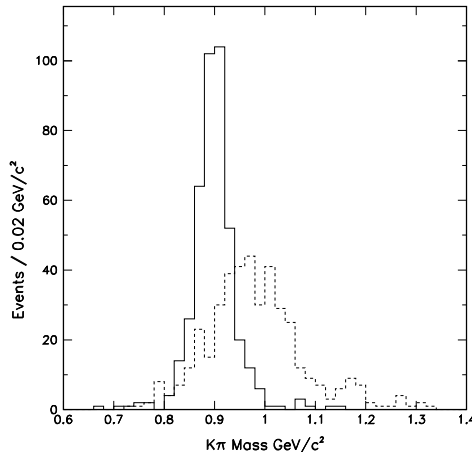


Figure 6. A Monte Carlo simulation for  $B \rightarrow K^* \gamma$  (solid) and  $B \rightarrow \rho \gamma$  (dashed) reconstructed as  $B \rightarrow K^* \gamma$ .

### 5.5.3. $\Delta\Gamma_s/\Gamma_s$

Browder *et al.* [20] show that if  $x_s = 15$ , a 7% difference in lifetime is expected. Several techniques can be used to determine  $\Delta\Gamma_{B_s}$  [21]. The statistical uncertainty on the  $B_s$  lifetime from semileptonic  $B$  decays in Run II will be well below 1%. With this constraint, the decay mode  $B_s \rightarrow J/\psi \phi$  can be decomposed into its two CP components (via a helicity analysis) fitting a separate lifetime for each component (if this final state is a pure CP eigenstate, its lifetime can simply be compared to the average  $B_s$  lifetime). Using Run Ia data, CDF has measured the helicity structure of the decays  $B \rightarrow J/\psi K^*$  and  $B \rightarrow J/\psi \phi$  [18]. In Run II, the  $B_s \rightarrow J/\psi \phi$  helicity structure should be known to about 1%, and the lifetime difference should be determined to 2-3%.

### 5.6. Rare $B$ decays

In Run I, CDF has performed a search for the decay modes  $B^\pm \rightarrow \mu^+ \mu^- K^\pm$ ,  $B^0 \rightarrow \mu^+ \mu^- K^{*0}$

and  $B_{d,s} \rightarrow \mu^+\mu^-$  [1]. Assuming the Standard Model Branching ratios [22] for  $B^+ \rightarrow \mu^+\mu^-K^+$  and  $B^0 \rightarrow \mu^+\mu^-K^{*0}$ , we expect in Run II  $\approx 400$   $B^+ \rightarrow \mu^+\mu^-K^+$  and  $\approx 650$   $B^0 \rightarrow \mu^+\mu^-K^{*0}$  events. This will enable us to study both (a) the invariant mass distribution of the dimuon pair and (b) the forward-backward charge asymmetry in the decay. Both of these distributions are sensitive to physics beyond the Standard Model, e.g. the presence of a charged Higgs or charginos [23], [24].

We also expect to observe the decays  $B^\pm \rightarrow e^+e^-K^\pm$  and  $B^0 \rightarrow e^+e^-K^{*0}$ . The decays  $B^\pm \rightarrow \ell^+\ell^+\pi^\pm$  and  $B^0 \rightarrow \ell^+\ell^-\rho^0$  are suppressed by an order of magnitude, but will be observable if we can achieve a high enough level of signal-to-noise. An observation of these decay modes would provide another determination of  $|V_{td}/V_{ts}|$ .

## 6. CONCLUSIONS

The CDF Run I has provided much experience in doing  $B$  physics at a hadron collider, including the reconstruction of  $B \rightarrow J/\psi K_s$ , and flavor tagging. This experience indicates that with an order of magnitude improvement in statistical sensitivity, we can obtain a competitive measurement of  $\sin(2\beta)$  in Run II. We expect to obtain this factor from accelerator upgrades, which will provide an order of magnitude more integrated luminosity, and detector upgrades, which will improve trigger and flavor tagging efficiency. Other  $B$  physics goals include the measurement of the CP asymmetry in  $B \rightarrow \pi^+\pi^-$ , the observation of  $B_s$  mixing, and high statistics observations of certain rare decay modes. Many fundamental measurements involve the  $B_s$ ,  $B_c$ , or  $\Lambda_b$ , and are thus complementary to  $B$  physics programs at the  $\Upsilon(4S)$ .

## REFERENCES

1. E. Meschi, this workshop.
2. M. Paulini, Proc. 6th Int. Symp. on Heavy Flavour Physics, Pisa, Italy (1995).
3. see <http://www-fermi3.fnal.gov/>
4. The CDF Upgrade, CDF/DOC/CDF/PUBLIC/3171.
5. Physics with CDF in Run II, CDF/DOC/CDF/PUBLIC/3172.
6. R. Aleksan, B.Kayser and P.Sphicas, Proc. of the Workshop on  $B$  physics at Hadron Accelerators, Snowmass, Colorado (1993).
7. M. Gronau and J.L. Rosner, Phys. Rev. **D49**, 254 (1994).
8. A. Ali, D. London, Z. Phys. **C65**, 431 (1995).
9. M. Ciuchini *et. al.*, Z. Phys. **C68**, 239 (1995).
10. Y. Nir, Proc. Workshop on  $B$  physics at Hadron Accelerators, Snowmass, Colorado (1993).
11. M.E. Lautenbacher, Proc. of the 27th Int. Conf. on High Energy Physics, Glasgow, Scotland (1994).
12. J.D.Lewis, J.Muller, J.Spalding, P.Wilson, Proc. Workshop on  $B$  physics at Hadron Accelerators, Snowmass, Colorado (1993).
13. N.G. Deshpande and X.G. He, Phys. Rev. Lett. **74**, 26 (1995).
14. F. DeJongh and P. Sphicas, FERMLAB-PUB-95/179-E.
15. D. Buskulic *et. al.*, Phys. Lett. **B356**, 409 (1995).
16. F. Abe *et al.*, Phys. Rev. Lett. **74**, 4988 (1995).
17. J. Skarha and A. B. Wicklund, Proc. of the Workshop on  $B$  physics at Hadron Accelerators, Snowmass, Colorado (1993).
18. F. Abe *et al.*, Phys. Rev. Lett. **75**, 3068 (1995).
19. The CLEO Collaboration, *Phys. Rev.* **D49** 5701, (1994).
20. T.E. Browder, S. Pakvasa, UH 511-814-95.
21. I. Dunietz, Phys. Rev. **D52**, 3048 (1995).
22. A.Ali, C.Greub, T.Mannel, Proc. of the ECFA Workshop on the Physics of the European B Meson Factory (1993).
23. A.Ali, T.Mannel and T.Morozumi, Phys. Lett. **B273**, 473 (1991); B.Grinstein, M.J.Savage and M.B.Wise, Nucl. Phys. **B319**, 271 (1989); W.Jaus and D.Wyler, Phys. Rev. **D41**, 3405 (1991).
24. A.Ali, G.Giudice and T.Mannel, Proc. of the 27th Int. Conf. on High Energy Physics, Glasgow, Scotland (1994).